Aust. J. Phys., 1982, **35**, 165–75

Observations of the Jupiter S-bursts between 3·2 and 32 MHz

G. R. A. Ellis

Department of Physics, University of Tasmania, G.P.O. Box 252C, Hobart, Tas. 7001.

Abstract

Observations of the Jupiter S-bursts in the frequency range 3·2–32 MHz are described. Their general properties including bandwidth, time duration, frequency–time behaviour, and rate of occurrence within this frequency range are analysed and discussed.

Introduction

The observation of very short pulses in the Jupiter decametric emissions was first reported by Kraus (1956) and Gallet (1961). The pulses, with a time duration of a few ms, were later called 'S-bursts'. It was shown by Warwick and Gordon (1965) and Riihimaa (1968) that they drift negatively in frequency, a property predicted by Ellis (1965) from a study of the analogous V.L.F. discrete emissions produced in the Earth's magnetosphere by monoenergetic electron streams (Dowden 1962; Ellis 1964). Most observations of the S-bursts have been made above 20 MHz, although they have been reported down to 3 MHz (Ellis 1975). It is the purpose of this paper to examine how their properties change over the frequency range 3·2–32 MHz.

Instrumentation

Observations were made between 2 and 18 MHz with a filled-aperture array of 2000 dipoles, 650 m × 650 m (Ellis 1972), located near Hobart, Tasmania. From 8 to 24 MHz a smaller array of orthogonal dipoles, 15 m × 30 m, provided information on the right- and left-handed circular polarization components, while above 24 MHz a second large filled-aperture array of 4096 dipoles, with an operating frequency range of 24–150 MHz, was used (Ferris *et al.* 1981). All three antennas were broadband in the sense that signals over the whole frequency range of each were simultaneously available at the antenna terminals.

The signals were divided into bands 3 MHz wide and recorded on eight video tape recorders, giving a total frequency range at any one time of 24 MHz. The telescopes were operated as transit instruments and the limited tape storage time restricted observations to 5 min at each transit of Jupiter, although the telescopes produced useful signals for a period of about 30 min or more. Future observations will be made using video casette recorders which, with their longer recording time, will permit observations limited only by the telescope beamwidths.

The tape-recorded R.F. signals were subsequently analysed using a 256-channel real-time spectrum analyser with a channel bandwidth of 10 kHz and a time resolution of 100 μs, the output being recorded on 35 mm film, with film speeds of up to 760

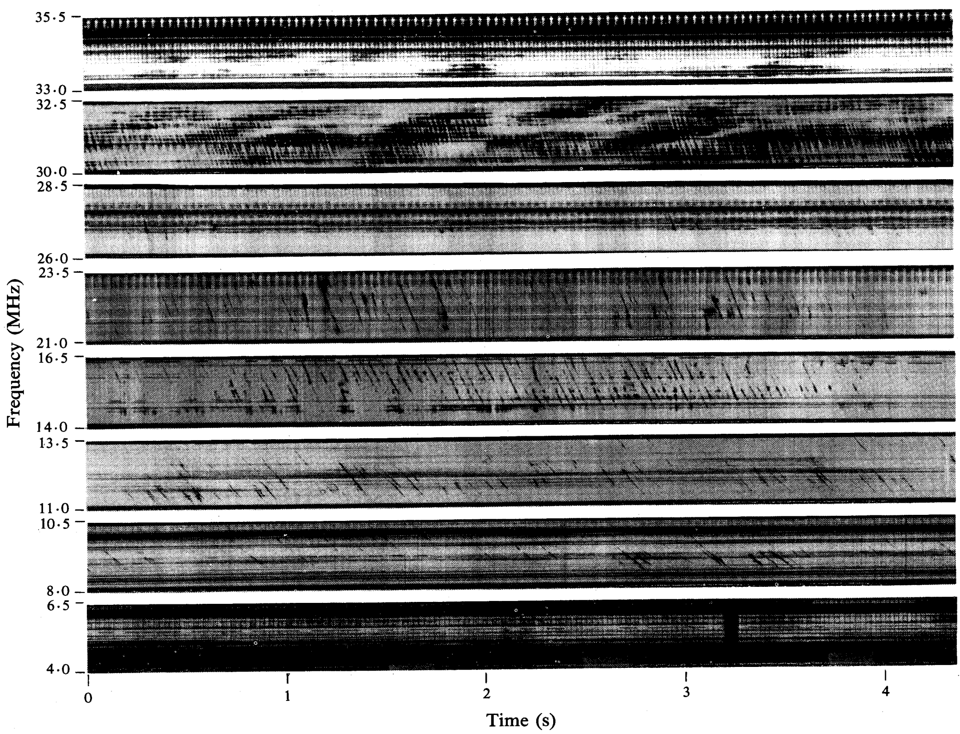

Fig. 1. Dynamic spectra of S-bursts in the frequency range 4–35 MHz, showing the increase in frequency drift rate with frequency.

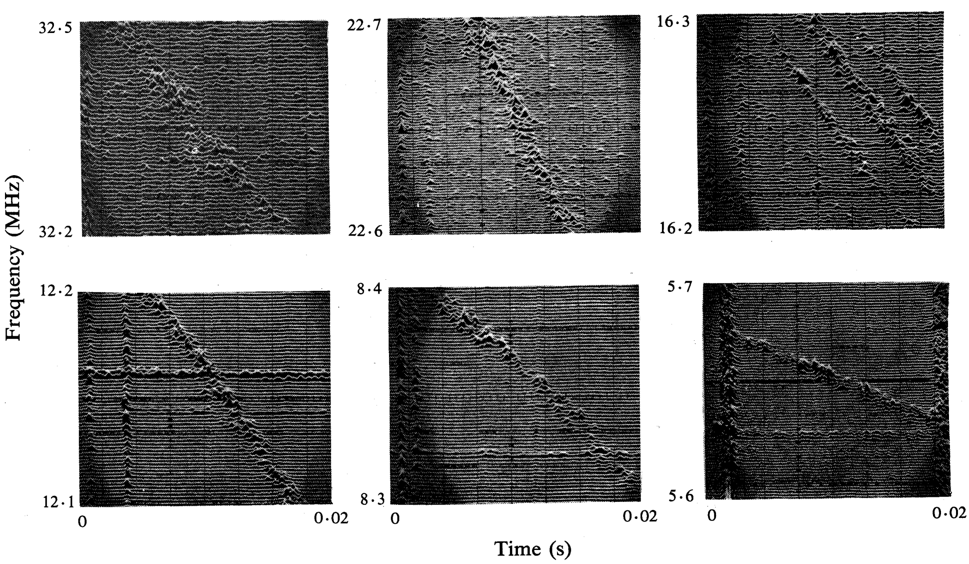

Fig. 2. Examples of spectra of individual S-bursts showing the variation of their bandwidth with frequency. (Note there is a change of frequency scale in the 32 MHz frame.)

cm min^{-1}. Selected bursts showing fine detail in the frequency–time plane were analysed with a time expansion spectrum analyser (Ellis 1973), with a frequency resolution of 2 kHz. In addition, some tapes were analysed with a second 256-channel spectrum analyser with a channel bandwidth of 100 kHz. This latter instrument was used in association with a bandwidth expander (Henry 1979), which increases the frequency range of input signals occupying a smaller bandwidth to match the 25·6 MHz bandwidth of the analyser. The effect is to produce a 256-channel analyser of variable frequency resolution and frequency range.

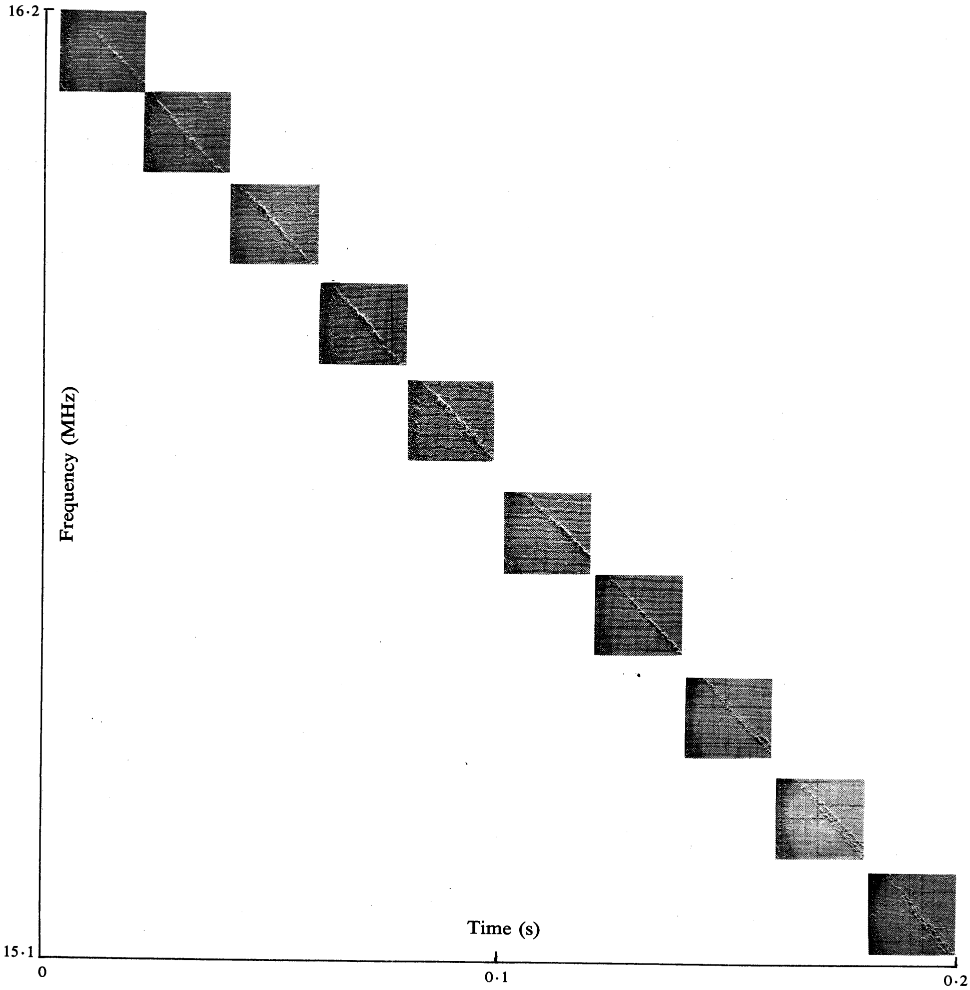

Fig. 3. Spectrogram of a complete single S-burst showing characteristic spreading and splitting in the frequency–time plane near the end of the trace.

Observations

Observations were made between 1972 and 1975 below 24 MHz, and from 1978 to 1980 between 24 and 34 MHz. Jupiter radio emissions were recorded during 154 transits out of 395 observed, and S-bursts were recorded on 62 of these. Representative spectra of the S-bursts in the frequency range 4–35 MHz are shown in Fig. 1 and illustrate their essential characteristics of narrow bandwidth, limited duration and rapid negative drift of frequency with time. Parts of spectrograms of individual bursts are shown enlarged in Fig. 2, and of a complete S-burst in Fig. 3.

Occurrence

Unlike the unstructured L-bursts, the S-bursts have been reported to be strongly correlated in their occurrence with the orbital position, i.e. superior geocentric conjunction (SGC), of the satellite Io for all wave frequencies down to 8 MHz (Whitham 1978). In the present observations this correlation was found to extend down to 3 MHz (Fig. 4).

The strong Io control of the bursts is shown in Fig. 5 where the central meridian longitude (CML) and SGC coordinates of all the S-bursts events between 22 and 3 MHz are shown. It is apparent from these observations that there is a weak correlation with CML, with a greater probability of observation where the SGC coordinate is near 090° and the CML near 200°, while there is a minimum in the occurrence rate where SGC ~ 240° and CML ~ 240° (see also Fig. 6).

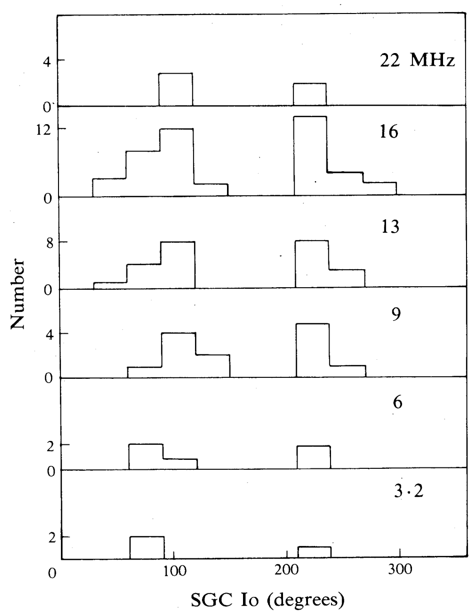

Fig. 4. Occurrence of S-bursts as a function of the SGC coordinate of Io.

Frequency Drift

The rate of change of wave frequency with time df/dt was found to vary from $\sim -30\ \mathrm{MHz\,s^{-1}}$ near 32 MHz to $\sim -1 \cdot 4\ \mathrm{MHz\,s^{-1}}$ near 3 MHz. Fig. 7 shows histograms of the magnitude of df/dt for different wave frequencies in this range for selected events, that is, for single transit observations. On any particular day, df/dt varied only slightly about its mean value for a particular wave frequency, with the ratio of the standard deviation to the mean being typically 0·1. A somewhat greater range of df/dt was observed over all transits and some correlation with the system III sub-Io longitude L was observed. This is illustrated in Fig. 8, where the individual points show the mean and standard deviation of df/dt for single events. The range of df/dt over different events was less for lower wave frequencies, and was also least where the Io longitude L was near 200° and greatest for L near 360°. The variation of df/dt is shown alternatively in Fig. 9 as a function of wave frequency for all events, with the observations for $180° \leq L < 260°$ (open circles) and $320° < L < 040°$ (solid circles) being plotted separately, the former showing consistently greater values.

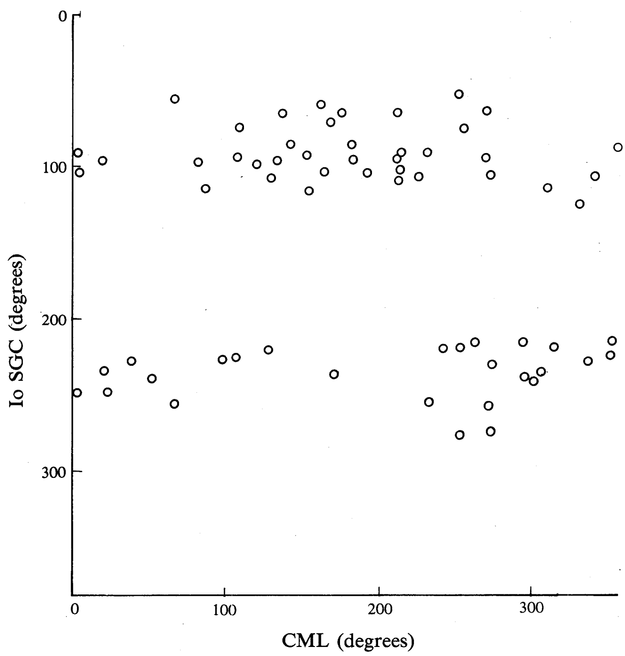

Fig. 5. Occurrence of S-bursts as a function of both the SGC coordinate of Io and the CML.

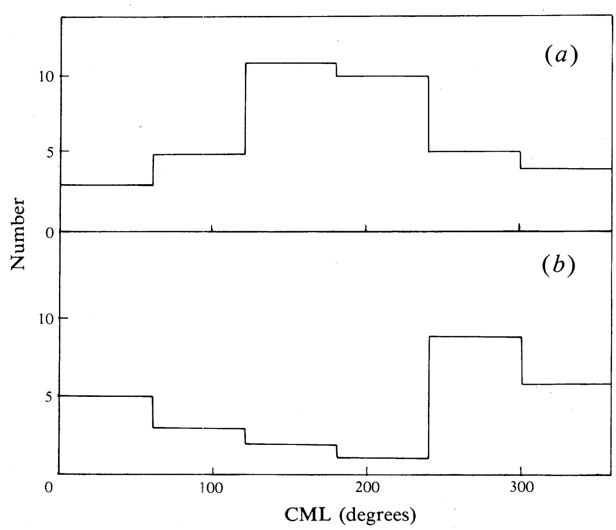

Fig. 6. Occurrence of S-bursts with CML for (a) SGC 060°–120° and (b) SGC 200°–260°.

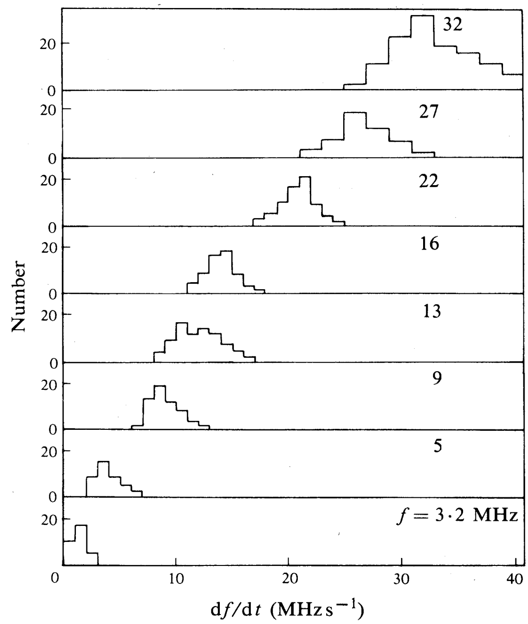

Fig. 7. Magnitude of frequency drift rate for individual S-burst events at different frequencies.

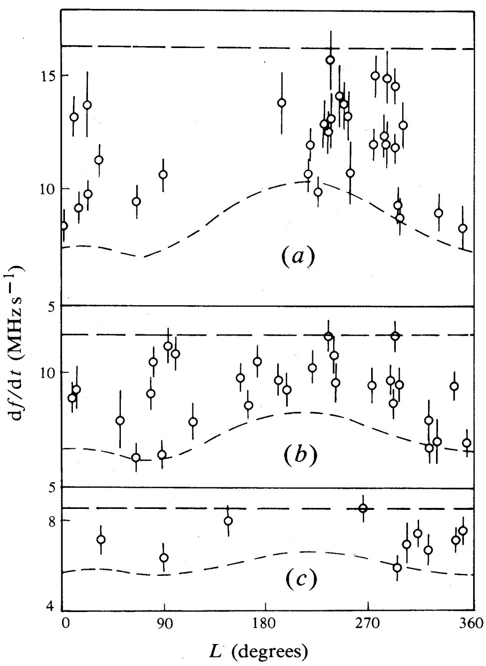

Fig. 8. Observed variation of df/dt of S-bursts with the system III longitude L of Io for wave frequencies of (*a*) 15 MHz, (*b*) 12 MHz and (*c*) 9 MHz. In each part the upper and lower dashed curves show the limits expected for df/dt with electron energy 3 keV and initial pitch angles 0 and $\frac{1}{2}\pi$ respectively (see p. 173).

Bandwidth, Time Duration and Frequency Limits

The instantaneous bandwidth of the bursts was observed to vary from $10\cdot5 \pm 2\cdot7$ kHz at $3\cdot2$ MHz to 49 ± 18 kHz at 32 MHz (Fig. 10). In the frequency range 5–16 MHz, the bandwidth of individual bursts were on many occasions less than the fre-

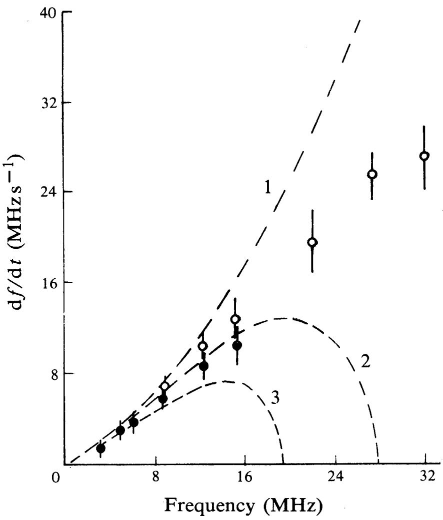

Fig. 9. Observed variation of df/dt with wave frequency from 3·2 to 32 MHz: solid circles, 320° < L < 040°; open circles, 180° < L < 260°. The dashed curves 1 and 2 show the calculated limits of df/dt for 320° < L < 040°, and 1 and 3 for 180° < L < 260°. Electron energy is 3 keV. (See p. 173.)

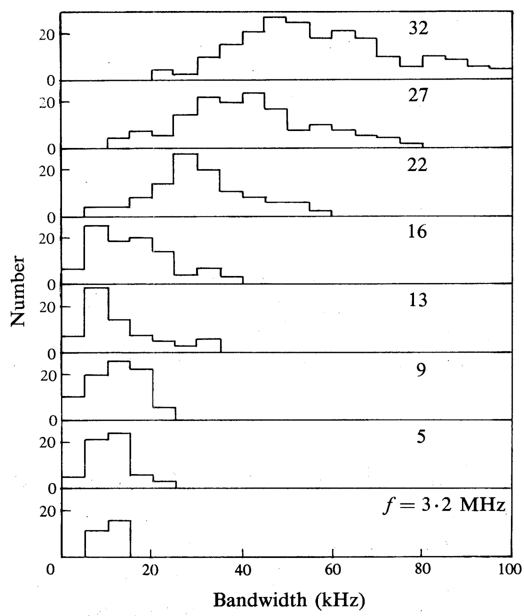

Fig. 10. Instantaneous bandwidth of S-bursts as a function of frequency.

quency resolution of the equipment (2 kHz). The single frequency time duration showed much less variation with frequency (Fig. 11), being near 2 ms for all frequencies except for those less than 6 MHz, where it increased rapidly to 13 ms at 3·2 MHz.

The overall frequency range Δf of individual bursts was normally relatively small (Fig. 12), with $\Delta f/f$ being typically 0·1, and decreasing slowly with frequency.

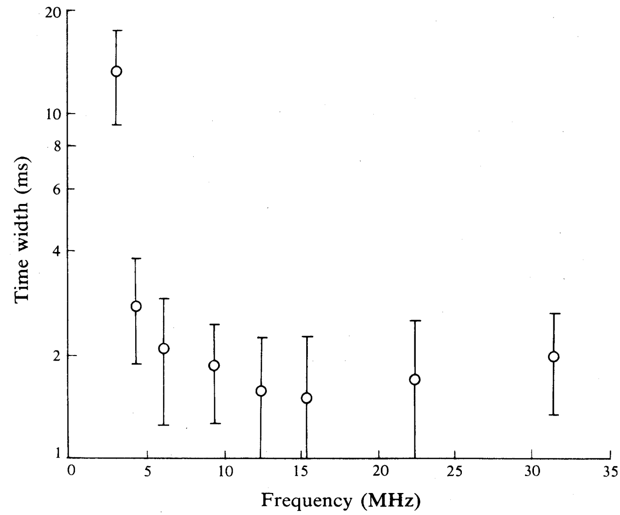

Fig. 11. Variation of single frequency time duration of S-bursts with wave frequency.

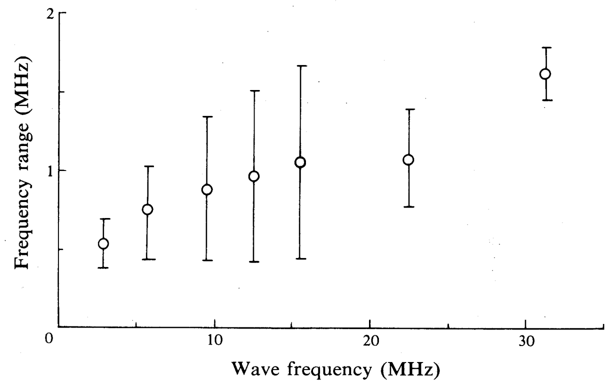

Fig. 12. Variation of the frequency range of S-bursts with wave frequency.

Discussion

Most theories of the S-bursts (Ellis 1965; Goldreich and Lynden-Bell 1969; Goldstein *et al.* 1981) assume that the radio emissions are generated by monoenergetic electron streams in the Jovian magnetosphere at a wave frequency approximately equal to the local cyclotron frequency. The rapid negative frequency drift has been taken to be produced by the motion of the source upwards through the magnetic field and simple calculations indicate that the electron energy would in this case be near 3 keV. A major source of the particle energy is apparently the unipolar induction produced by the satellite Io in its relative orbital motion across the Jovian magnetic field (Goldreich and Lynden-Bell 1969). In addition, the close correlation observed between the occurrence of the S-bursts and the SGC coordinate of Io (Fig. 4) for all wave frequencies may be accounted for if the electrons responsible for the S-bursts as distinct from other types of bursts are all confined to the Io flux tube (IFT) (Whitham 1978; Ellis 1980). The SGC correlation then follows if the radiation is emitted in a conical shell pattern of semi-angle near 80°, the radiation then being observable only when Io is either side of Jupiter. This pattern of radiation is characteristic of most theories of the emission (Ellis and McCulloch 1963; Ellis 1965; Goldstein *et al.* 1981).

The frequency drift is always negative except for some unusual bursts observed below 10 MHz (Ellis 1975) and, to account for the apparent upward motion of the observed radiating electrons and the narrow bandwidth of the bursts, it has been suggested that the electrons emerge with uniform energy and pitch angle from the turbulent region at the foot of the IFT within the Jupiter ionosphere where the current circuit of the electrons accelerated at Io is completed (Whitham 1978; Desch *et al.* 1978; Ellis 1980). If it is assumed that the pitch angle of the electrons may range from 0 to $\frac{1}{2}\pi$ at the foot of the IFT, and that the energy is always 3 keV, then the variation of df/dt both with Io longitude L and with frequency, illustrated in Figs 8 and 9 respectively, follows from the variation of the Jovian magnetic field as the planet rotates under Io (Ellis 1980). The surface magnetic field intensity B_0 along the track of the foot of the IFT is least for longitudes near 360° and greatest near 200°, and the ratio of the magnetic field in the foot to that at the height of radio emission at a particular frequency is hence least and greatest for these two longitudes respectively.

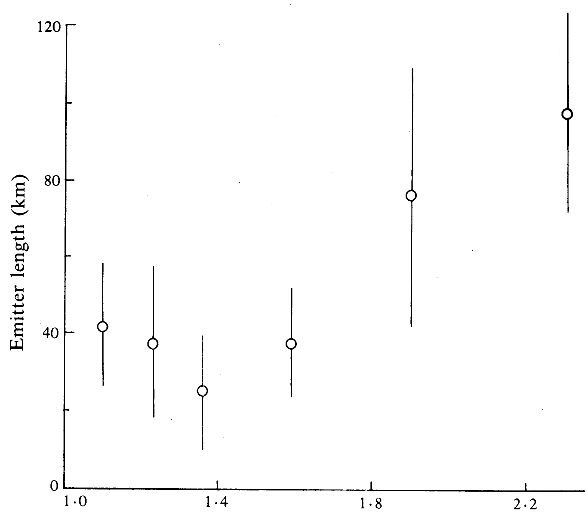

Fig. 13. Variation with radial distance (R_J is the Jovian radius) of the longitudinal extent of the source region of the S-bursts calculated from their bandwidth.

The longitudinal velocity of the electrons at the point of observed S-burst emission will depend only on their initial pitch angle ϕ_0 and on B_0, that is,

$$df/dt = -KV_{\parallel} = -KV\{1-(B/B_0)\sin^2\phi_0\}^{\frac{1}{2}},$$

where K is a constant and B is the magnetic field at the emission point. The maximum and minimum values of df/dt obtained by taking $\phi_0 = 0$ and $\frac{1}{2}\pi$ will vary with wave frequency f ($\propto B$) and with B_0, and hence the Io longitude L. Fig. 8 shows the variation with L of the limits of df/dt calculated in this way for wave frequencies 9, 12 and 15 MHz. In Fig. 9 the same limits are shown for the two restricted longitude regions specified earlier. Both northern and southern hemisphere values of B_0 were used since polarization observations (Whitham 1979) have shown that S-bursts below 17 MHz may have either right- or left-handed polarization and may presumably originate in either hemisphere. It can be seen that all the observed values of df/dt fit reasonably well between the limits calculated using an electron energy of 3 keV, whether they are plotted as a function of frequency or of Io longitude.

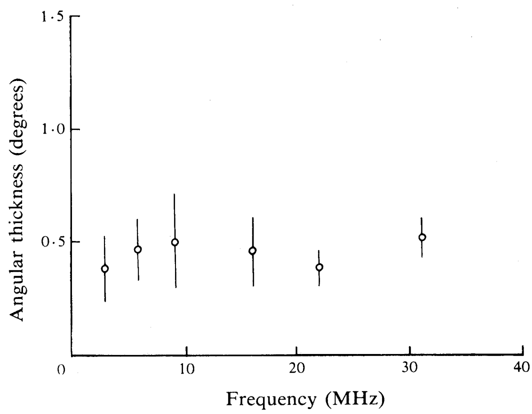

Fig. 14. Calculated thickness of the conical shell emission pattern at various frequencies.

The instantaneous bandwidth of the bursts defines an upper limit to the length of the radiation source in the magnetic field direction if the wave frequency is taken to be approximately the cyclotron frequency, since this will vary spatially with the magnetic field. From the bandwidth observations of Fig. 10, the variation of emitter length with radial distance from Jupiter is found to be in the range 25–100 km for observations between 3·2 and 32 MHz (Fig. 13).

The overall frequency range of individual S-bursts of $\sim$1 MHz (Fig. 12) may be accounted for by motion of the source along the curved magnetic field line, so that the thin edge of the emission cone sweeps past the observer. In this case the frequency range of the bursts may be used to determine the angular thickness of the emission cone, and Fig. 14 shows how this derived quantity varies with frequency. An angular thickness of $\sim 0{\cdot}5°$ would account for the frequency limits of the bursts over the whole frequency range of the observations.

Acknowledgments

This research was supported financially by the Australian Research Grants Committee and the Australian Radio Research Board.

References

Desch, M. D., Flagg, R. S., and May, J. (1978). *Nature* **272**, 38.
Dowden, R. L. (1962). *J. Geophys. Res.* **67**, 1745.
Ellis, G. R. A. (1964). *Aust. J. Phys.* **17**, 63.
Ellis, G. R. A. (1965). *Radio Sci.* D **69**, 1513.

Ellis, G. R. A. (1972). *Proc. Astron. Soc. Aust.* **2**, 135.
Ellis, G. R. A. (1973). *Aust. J. Phys.* **26**, 253.
Ellis, G. R. A. (1975). *Nature* **253**, 415.
Ellis, G. R. A. (1980). *Nature* **283**, 48.
Ellis, G. R. A., and McCulloch, P. M. (1963). *Aust. J. Phys.* **16**, 380.
Ferris, R. H., Turner, P. J., Hamilton, P. A., McCulloch, P. M., and Ellis, G. R. A. (1981). A broadband phased array. Radio Research Board Seminar on Array Beamforming, Adelaide.
Gallet, R. M. (1961). *In* 'Planets and Satellites' (Eds G. P. Kemper and B. M. Middlehurst) (Univ. Chicago).
Goldreich, P., and Lynden-Bell, D. (1969). *Astrophys. J.* **156**, 59.
Goldstein, M. L., Sharma, R. R., Ben-Ari, M., Eviatar, A., and Papadipoulos, K. (1981). A theory of Jovian decameter radiation. Univ. Maryland Preprint.
Henry, P. S. (1979). *Rev. Scient. Instrum.* **50**, 185.
Kraus, J. D. (1956). *Astron. J.* **61**, 182.
Riihimaa, J. J. (1968). *Nature* **218**, 1141.
Warwick, J. W., and Gordon, M. A. (1965). *Radio Sci.* D **69**, 1537.
Whitham, P. S. (1978). *Nature* **272**, 40.
Whitham, P. S. (1979). Ph.D. Thesis, University of Tasmania.

Manuscript received 23 November 1981, accepted 26 February 1982